



An Improved Local Geoid Model for Egypt using Satellite Geopotential and Terrestrial Data

Mohamed El-Ashquer¹, Basem Elsaka^{2,3}, and Gamal El-Fiky¹

(1) Construction Engineering and Utilities Department, Faculty of Engineering, Zagazig University, Zagazig, Egypt.

(2) National Research Institute of Astronomy and Geophysics (NRIAG), Helwan, Cairo, Egypt.

(3) Institute of Geodesy and Geoinformation, University of Bonn, Nussallee 17, 53115, Bonn, Germany.

الملخص العربي

نظرا لأهمية رسم الخرائط وأعمال المساحة والجيوديسيا ومشاريع البنية التحتية الكبيرة فوجود نموذج للجيونيد المحلي الدقيق لمصر أمر ضروري لتحويل الإرتفاعات الجيوديسية المسندة الى سطح الألبسويد والمقاسة عن طريق النظام العالمي لتحديد الموقع إلى الإرتفاعات الأرثومترية والمسندة الى سطح الجيونيد.

الهدف من البحث الحالى هو استخدام أفضل نموذج من النماذج العالمية لحساب الجيونيد التى يتم الحصول عليها من القمر الصناعى GOCE الذى أطلق من كاله الفضاء الأوربييه فى عام ٢٠٠٩ بهدف قياس شذوذ الجاذبية الأرضية بدقة ١- 2 مللى جال وتحديد الجيونيد بدقة ١-٢ سم . لإنتاج نموذج محسن لمستوي سطح الجيونيد لمصر "EGY-HGM2016" تم إستخدام طريقة أقل المربعات التجميعية (LSC) لإجراء عملية الحذف- والأستعاد (RCR). بالإضافة الى هذا استخدمت البيانات الجيوديسية المتاحة من أرصاد نظام تحديد المواقع العالمى بأرصاد الميزانية (GPS/levelling) ونقاط شذوذ الجاذبية الأرضية ونموذج إرتفاعات رقمي "SRTM 30+" وذلك لتمثيل طبيعة تضاريس سطح الأرض المحلى لجمهورية مصر العربية. وقد تم تقييم الجيونيد "EGY-HGM2016" المستنتج بأستخدام مقارنه أرصاد نظام تحديد المواقع العالمى بأرصاد الميزانية (GNSS/levelling) و النماذج العالمية لحساب الجيونيد EGM2008. ولقد أشارت نتائج البحث إلى أن مستوى انحراف معيارى للفرق بين "EGY-HGM2016" و أرصاد نظام تحديد المواقع العالمى بأرصاد الميزانية (GPS/levelling) هو 19.7 سم بالمقارنة بحالة بالنماذج العالمية لحساب الجيونيد EGM2008 الانحراف المعيارى 48سم.

Abstract

An improved hybrid gravimetric geoid model for Egypt, HGM2016, has been recently computed implementing the least squares collocation (LSC) method through the Remove-Compute-Restore (RCR) procedure. The computation of HGM2016 involves different datasets in terms of gravity anomalies determined from the GOCE-based global geopotential model (SPW-R4) up to d/o 200 and EGM2008 up to d/o 201 to 720 combined with terrestrial gravity datasets in terms of 2140 gravity field anomalies and about 121480 marine surface gravity anomalies. In addition, orthometric heights from 17 GPS/levelling measurements have been considered during the modelling process to improve the determination of the local gravimetric geoid over the Egyptian region.

HGM2016 model estimated over Egypt result geoid heights that are ranging from 7.677 m to 21.095 m of standard deviations (st. dev.) of about 2.534 m in the northwest of the country excluding the involvement of the orthometric heights from GPS/levelling measurements. When the later dataset is considered during the implementation of LSC process, hybrid residual height anomalies ranging from -1.5 m to +0.9 m, with mean 0.22 m and st. dev. 0.17 m are obtained. Comparison of the predicted local gravimetric geoid with the corresponding ones obtained from EGM2008,

GOCE-based SPW R4 model, and GPS/Levelling reveals considerable improvements of our HGM2016 model over Egypt.

Keywords

Hybrid Local Geoid Model – Remove-Compute-Restore (RCR) – Least Square Collocation (LSC)

1. Introduction

Gravimetric geoid determination from dense datasets such as surface gravity, global geopotential models (GGMs) and topography is widely applied on both regional and local scales (see e.g. Denker et al., 2000; Smith and Roman, 2001). The current models over Egypt recover the regional/local geoid accurately at short wavelengths, however they may suffer from systematic errors in longer wavelengths due to errors of the geopotential model and/or truncation procedures such as EGG97 (Denker et al., 2000), JGEOID2000 (Kuroishi, 2001b) and GEOID93 (Milbert, 1995). On the other hand, orthometric heights determined from GPS/levelling measurements give precisely point-wise geoid undulations, which contain the full range of geoid signals, but do not actually give the geoid heights in a strict sense. Therefore, the determination of gravimetric geoid undulations is highly required.

A reliable geoid model in terms of spatial resolution and accuracy should be determined using the available gravimetric information combined with GPS/levelling geoid undulations (see e.g. Smith and Milbert, 1999).

In this contribution, hybrid gravimetric geoid model over Egypt could be computed by combining ground-based gravity and GPS/levelling observations using remove-compute-restore (RCR) technique (similar to Schwarz et al., 1990) to obtain a developed conversion surface that effectively warps the gravimetric geoid surface (using least squares collocation) by fitting the GPS/levelling points. Finally, gravimetric geoid undulations endeavor to model the geoid as possible. For the Egyptian region, a number of studies has been published using different quasi-geoid determination methods (Alnaggar, 1986; El-Tokhey, 1993; Nassar et al., 2002; Dawod, 2008; Abd-Elmotaal, 2008). However, this study differs from the previous studies in that, identical input gravity anomalies have been incorporated from the recently released model GO_CONS_GCF_2_SPW_R4 (Gatti et al., 2014), up to maximum degree and order (d/o) 200 which is based on GOCE (Gravity field and steady-state Ocean Circulation Explorer) mission observations.

We have to mention here that the GOCE-based GGM of type SPW_R4 (up to SH d/o 200) was suggested to be used as a reference geopotential model when modeling the local gravimetric quasi-geoid, since it approximates the gravity field well the over Egypt (El-Ashquer et al., 2016). Moreover, short wavelength of the gravity spectrum was compensated using EGM2008 (Pavlis et al., 2012) from d/o 201 to d/o 720.

For our model computations, the GRAVSOFTE software package (Forsberg and Tscherning, 2008) has been used. In the following, the datasets used in our calculations are briefly described in Section 2. In Section 3, methodology and procedures for computing the hybrid gravimetric geoid model are discussed. The accuracy assessment of hybrid gravimetric geoid/quasigeoid model is given in Section 4. Finally, conclusions are outlined in Section 5.

2. Datasets

The datasets used in this study consist of: (1) GOCE-based and EGM2008 geopotential gravity models, (2) terrestrial free-air gravity anomalies and GPS/levelling data collected over the Egyptian region, (3) shipborne marine gravity data and DTU 2013 and (4) High-resolution topographic data from the SRTM30_PLUS (Shuttle Radar Topography Mission) digital terrain model. Figure 1 shows the distribution of the different dataset used in this study.

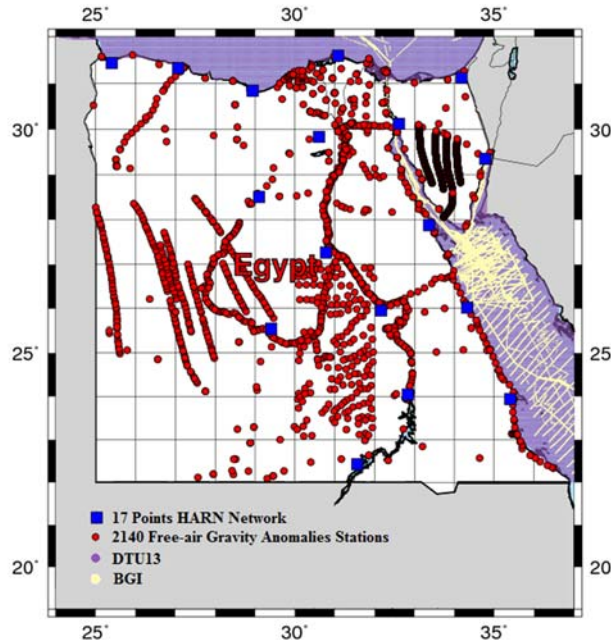


Figure 1: Distribution of available datasets for Egypt used in the current study.

2.1. Free-air terrestrial gravity data

The available gravity dataset in this study consists of 2140 point stations. The distribution of gravity data is not homogeneous over Egypt, with significant gaps, particularly in the eastern and western deserts (Dawod et al., 2008). Therefore rough data were reduced then filtered by rejecting the data subjected to gross errors. Among gravity observations (i.e. 2140 stations) prior to the cross validation (XV), 111 stations could not meet the XV conditions. So, after XV process, 2029 available gravity point stations have been applied to our study, Table 1 show the statistics of the gravity field observations in terms of free-air anomalies before and after XV process.

Table 1: Statistics of terrestrial and marine gravity anomalies used in this study before and after the cross validation (XV) process [mGal].

XV	Population	Min	Max	Mean	st. dev.
Terrestrial gravity anomalies (Before)	2140	-102.69	96.13	-10.75	22.74
Terrestrial gravity anomalies (After)	2029	-97.31	78.63	-11.11	22.09
Marine gravity anomalies (BGI + DTU13)	121480	-201.248	110.384	-17.812	34.336

2.2. Marine Gravity Data

Marine gravity data incorporates terrestrial shipborne (sea surface land and sea bottom), and altimetric gravity field (i.e. based on satellite altimetry). Indeed, we couldn't succeed to obtain any of the marine data from sources in Egypt. Bureau Gravimetrique International (BGI), whose objectives are to collect, compile and store on a worldwide basis, homepage is <http://bgi.omp.obs-mip.fr/data-products/Gravity-Databases/Marine-Gravity-data> supplied us with 64138 records shipborne marine gravity anomalies for almost the whole area surrounding Egypt. The satellite altimetry is the second source of our marine gravity data provided by DTU13 global marine gravity filed (Anderson and Knudsen, 2013) in form of 1' x 1' grid gravity anomaly data covering the Mediterranean Sea and Red Sea surrounding Egypt. During XV process, 8851 stations were duplicated and could not meet the XV conditions, most probably due to the smoothing effect of the big gap size compared to the DTU13; however, we have cross validated all marine dataset, which amount to 121480 records. The statistics of marine gravity before and after XV are given in Table 1.

2.3. GPS/levelling data

GPS/levelling dataset available here consists of 17 stations of the Egyptian National High Accuracy Reference Network (HARN) observed by the Egyptian Survey Authority to form the New Egyptian Datum 1995 (NED-95), distributed over Egypt (see Figure 1). In this network, the GPS observations were tied to the International Geodetic Stations (IGS) reference system. The precision of geoid undulations at these stations has been suggested from the provider of about 1 cm or lower. Despite the fact that the distribution of the GPS/levelling dataset of 17 stations is rather sparse, one may use them for the assessment purpose since these stations cover almost the Egyptian territory in different areas (Dawod et al., 1998).

2.4. High-resolution terrain data

The SRTM30_PLUS (Shuttle Radar Topography Mission of spatial resolution about ~900 m, 30 arc-sec) data is used in this study to compute the topographic potential effect on the geoid over Egypt.

3. Methodology and Computation

The remove-restore principle (see Hofmann and Moritz, 2005, p. 379) is considered as one of utilized methods in geodesy to remove the trends of the mean-static gravity signal (i.e. long wavelength gravity spectrum from the earth gravity models) (Δg_{GGM}) from the raw gravity anomalies (Δg_{Fa}), and after collocation process, to restore the effect again on the result. This step is done using GGM module of the GRAVSOFIT. Similarly, the gravity effect due to the topographic attraction representing the very-short wavelength component (Δg_{RTM}) has been removed from the raw gravity anomalies (Δg_{Fa}) to compute finally the resulting residual anomalies (Δg_{res}) as

$$\Delta g_{res} = \Delta g_{Fa} - \Delta g_{GGM} - \Delta g_{RTM} \quad [1]$$

Table 2 shows the statistics of Eq. [1] representing the residual gravity anomalies. It shows clearly that removing the long wavelength components (Δg_{GGM}) from the free-air gravity anomalies (Δg_{Fa}) yields substantial smoothing as indicated by the reduction of

standard deviations (st. dev.) of about 46%. Slight refinements in terms of minimum and maximum of the anomalous residual gravity (Δg_{res}) were expected after removing the very-short wavelength components due to local topography. This might be due to the poor quality of available free-air gravity anomalies over Egypt, since the topography is very smooth (i.e. flat areas) in the major area of Egypt.

Table 2: Statistics of residual gravity anomalies [mGal]

Anomaly	Min	Max	Mean	st. dev.
Δg_{Fa}	-201.24	110.38	-17.70	34.18
$\Delta g_{Fa} - \Delta g_{GGM}$	-168.88	107.62	-3.39	18.16
$\Delta g_{Fa} - \Delta g_{GGM} - \Delta g_{RTM}$	-166.51	73.64	-12.17	19.93

So, residual anomalous gravity field (Δg_{res}) has been used to compute the isotropic empirical covariance function via the EMPCOV program of the GRAVSOFIT. To estimate such an isotropic covariance function empirically; a spherical distance ψ is suitably chosen and the product sum average of pairs of anomaly values, relevant to pairs of points having spacing ψ with the condition that $(\Delta\psi/2) \leq \psi \leq \psi + (\psi/2)$, is to be evaluated (Tscherning and Rapp, 1974). In the current study, $\Delta\psi$ was chosen to be 15 arc-minutes. The obtained results of the empirical covariance function are identical to those calculated by the modelled (or analytical) covariance function using the analytical Tscherning/Rapp model (ibde). The latter covariance function is required to perform the computations through the LSC method, where the required auto- and cross-covariance functions are computed by covariance propagation from the analytically modelled local covariance function represented as follows:

$$\text{cov}(T(P), T(Q)) = \alpha \sum_{n=2}^{N_{\max}} \sigma_n^2 \left(\frac{R_E^2}{r_P r_Q} \right)^{n+1} P_n(\cos \psi) + \sum_{n=0}^{\infty} = N_{\max} + 1 \frac{A}{(n-1)(n-2)(n-4)} \left(\frac{R_B^2}{r_P r_Q} \right)^{n+1} P_n(\cos \psi) \quad [2]$$

Where P and Q are two points separated by a spherical distance ψ and r_P, r_Q are the distances of the two points from the geocenter, R_B is the radius of Bjerhammar sphere and σ_n^2 is the error degree variance. The covariance parameters α (scale parameter), A (a constant parameter in units of $(\text{m/s})^4$) and R_B are determined using an iterative non-linear adjustment, which based on the local residual gravity anomaly data, via its empirical covariance function used as input for the collocation process (Knudsen, 1987).

The following covariance parameters were then obtained and applied into the collocation process: the depth to the Bjerhammar sphere $R_B = -4.30037$ km, the variance of gravity anomalies at zero altitude of 248.18 mGal^2 , the error degree variance scale factor of 2.7956, and $N_{\max} = 720$. These estimated parameters were used to calculate the hybrid residual height anomalies on $15' \times 15'$ grid from the residual gravity anomalies.

Now we can predict hybrid residual height anomalies at the Earth's surface ($\delta\zeta_{res}$) by using both the reduced gravity data (Δg_{res}) and the reduced height anomalies (ζ_{res}). For this step, the residual height anomalies from the reduced gravity anomalies (Δg_{res}) are computed at points of GPS/levelling data. The comparison between predicted residual height anomalies from the reduced gravity anomalies (Δg_{res}) and observed (from GPS/levelling) residual height anomalies (ζ_{res}) is shown in Table 4. The results show differences between the predicted and observed height anomalies with an error st. dev. of about 42 cm. So, we ran the collocation process again taking the error estimates (about 1.49 cm in terms of st. dev.) into consideration to remove the bias between both the predicted and observed height systems (i.e. the gravimetric and geometric, respectively).

Table 4: Statistics of predicted and observed height anomalies (m) at GPS/levelling stations.

Anomaly	Observations	Predictions	Difference	Error Estimates
Mean	0.2869	0.0548	0.2321	0.1115
St.Dev	0.4169	0.1507	0.4294	0.0149
Max.	0.9242	0.4020	0.8048	0.1293
Min.	-0.5255	-0.2227	-0.6078	0.0756

The comparison between predicted residual height anomalies from the reduced gravity anomalies (Δg_{res}) and observed (from GPS/levelling) residual height anomalies (ζ_{res}) after removing the bias (where the mean of differences became 0.0 m) over the 17 GPS/levelling is shown in Table 5. The result shows that we are able to predict residual height anomalies of about 7.8 mm in terms of st. dev. of the differences.

Table 5. Statistics of predicted and observed height anomalies (m) at GPS/levelling stations after removing the bias between both height systems.

	Observations	Predictions	Difference	Error Estimates
Mean	0.2869	0.2869	0.0000	0.0554
St.Dev.	0.4169	0.4098	0.0078	0.0001
Max.	0.9242	0.9188	0.0114	0.0555
Min.	-0.5255	-0.5051	-0.0203	0.0550

The residual gravity data remained at all the data points together with their computed covariances were then used in the geoid collocation process, utilizing the law of variance-covariance propagation, and the residual height anomalies (ζ_{res}) from GPS/levelling after removing the bias via the LSC method to estimate the hybrid residual height anomalies ($\delta\zeta_{res}$), and their error estimates. Afterwards, the effects of both removed parts (i.e. the long (ζ_{GGM}) and short wavelength (ζ_{RTM}) components, see Eq. [1]) were then restored and were added to the 'predicted' residual height anomaly ($\delta\zeta_{res}$), at the computation points to get the final hybrid height anomaly ζ_H values as

$$\zeta_H = \zeta_{GGM} + \delta\zeta_{res} + \zeta_{RTM} \quad [3]$$

The computation of the hybrid gravimetric quasigeoid model has been performed using the GRAVSOF modules GEOEGM, TC, EMPCOV, COVFIT and GEOCOL (Forsberg and Tscherning, 2008). Figure 2 shows a scheme of the computation steps of

the hybrid gravimetric geoid-quasigeoid model on the basis of free-air gravity anomalies, the GGM and the DEM.

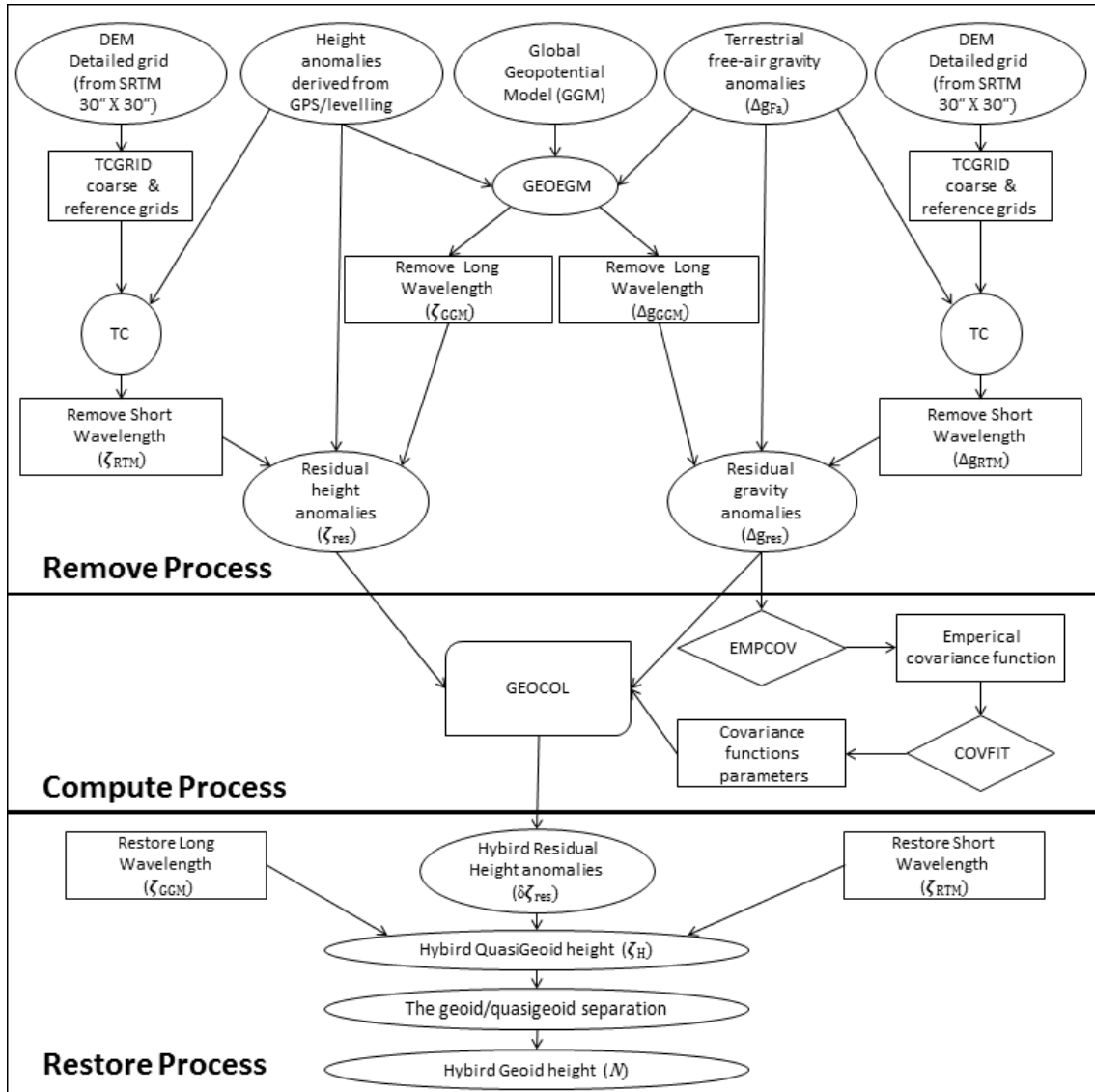
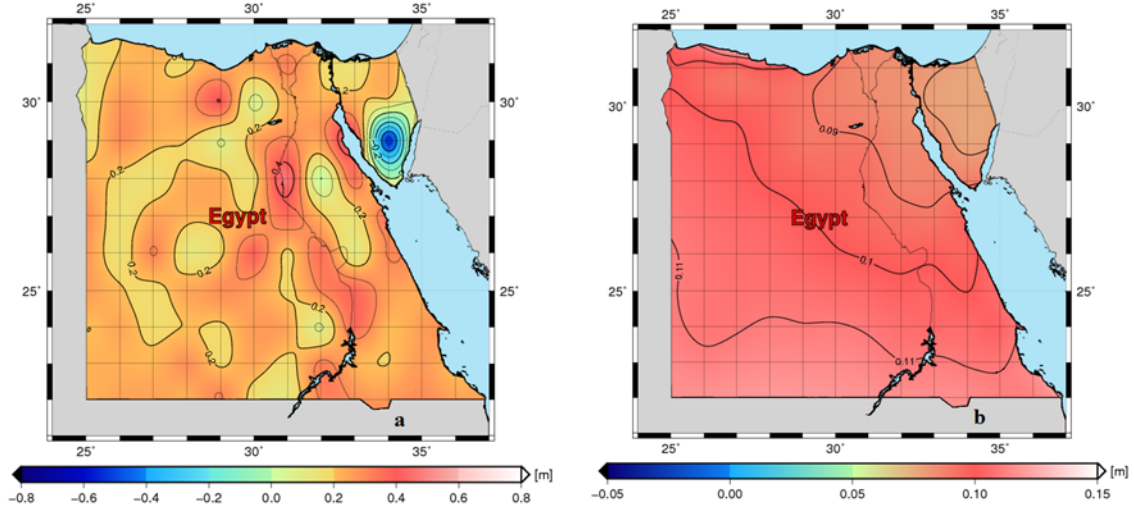


Figure 2: Flowchart illustrating computation of the hybrid gravimetric geoid- quasigeoid model based on free-air gravity anomalies derived from ground-based, GGM and DEM data with the consideration of height anomalies derived from GPS/levelling.

Indeed, we have to mention that we have used free-air gravity anomalies refer to ground level and telluroid (Hofmann and Moritz, 2005), whereas the conventional gravity anomalies have been referred to sea level. This means that we have not yet estimated the geoid heights but the quasigeoid or height anomaly (ζ). Separation due to the conceptual difference between the geoid and the quasigeoid is expressed as (ibde. p. 325).

$$N - \zeta \approx \frac{\Delta g_B}{\bar{\gamma}} H \quad [4]$$



Where Δg_B is the Bouguer anomaly, $\bar{\gamma}$ is the mean normal gravity, and H is the elevation above the sea level in the same units as N and ζ .

$$N \approx \zeta + \frac{\Delta g_B}{\bar{\gamma}} H \quad [5]$$

The hybrid gravimetric quasigeoid model EGY-HQGM2016 was computed by restoring the reference height anomalies ζ_{GGM} , and the corresponding ones from topography effects ζ_{TRM} . Consequently, both quantities were added to the residual height anomalies $\delta\zeta_{RES}$ (see Eq. [3]). Finally, the hybrid gravimetric quasigeoid model EGY-HQGM2016 has been converted to the hybrid gravimetric geoid model HGM2016 based on Eq. [5].

Figure 3 shows the different estimated components used to restore the hybrid gravimetric geoid- quasigeoid model. The hybrid residual height anomalies $\delta\zeta_{RES}$ is indicated in Figure (3a), whereas, Figure (3b) shows that the error accuracy of the computations of $\delta\zeta_{RES}$ is ranging from 6 cm to 16 cm with mean values of about 9 cm and standard deviation 1.4 cm.

The major contribution to the gravimetric geoid model in Figure (3c) comes from the reference geoid model ζ_{GGM} obtained from modified GGM truncated to d/o 720. Figure (3d) represents the height anomalies restored from the topography effect ζ_{RTM} , which range from -18 cm to 40 cm with a mean of about -1.3 cm over Egypt.

The hybrid gravimetric quasigeoid model EGY-HQGM2016 is then indicated in Figure (3e). The geoid/quasigeoid separation indicated in Figure (3f) is at the level of 1 cm for the majority of the Egyptian territory reaching up to -39 cm in the mountains.

Finally, the hybrid gravimetric geoid model HGM2016 as given in Figure 4 is obtained by adding geoid/quasigeoid separation (Fig. 3f) to the hybrid gravimetric quasigeoid model EGY-HQGM2016 (Fig. 3e).

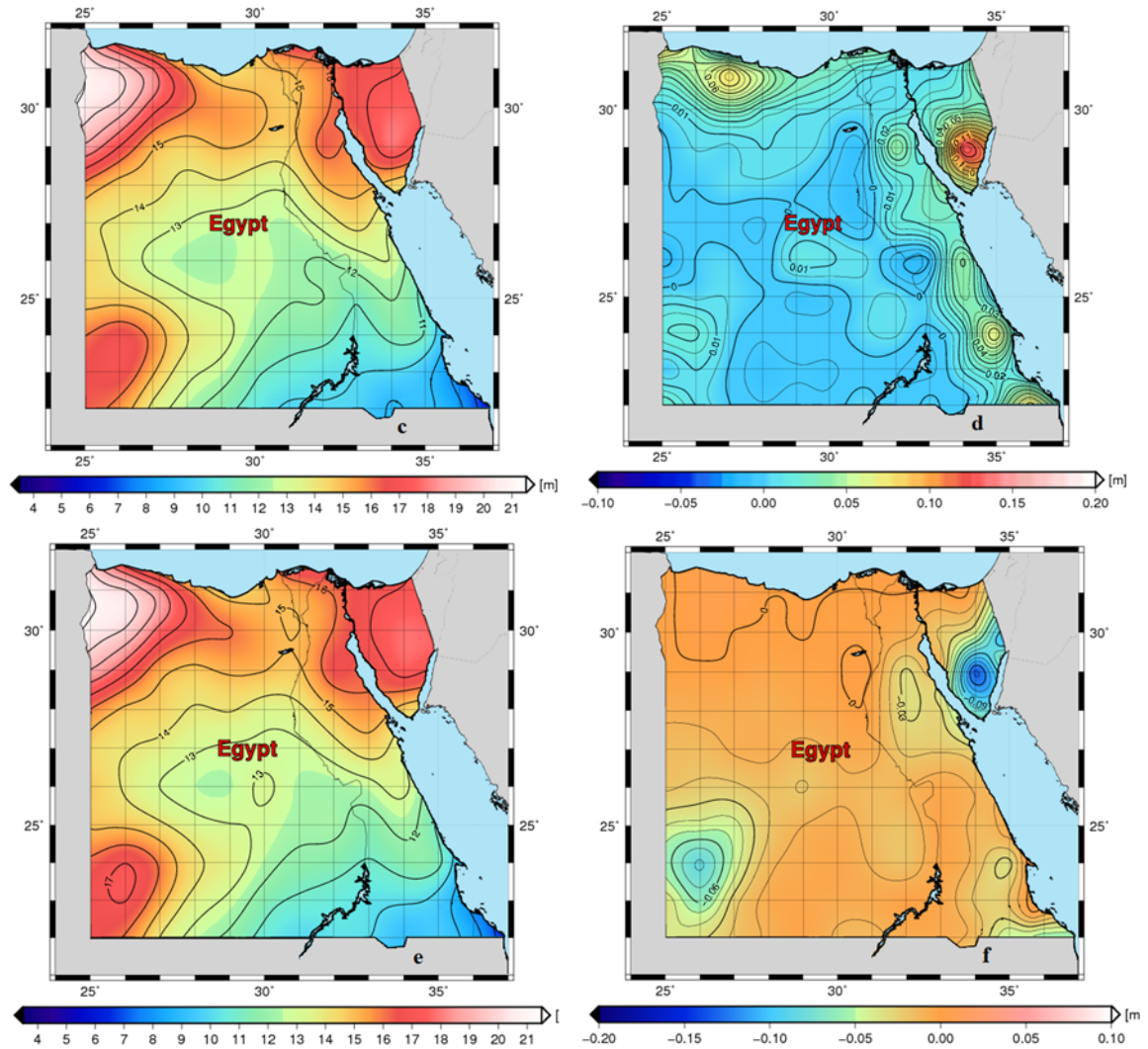


Figure 3: (a) The hybrid residual height anomalies, (b) error accuracy of hybrid residual height anomalies, (c) the reference height anomalies, (d) RTM effects on height anomalies, (e) hybrid gravimetric quasigeoid model EGY-HQGM2016, and (f) geoid-to-quasigeoid separation [m].

Table 3 shows the statistics hybrid gravimetric quasigeoid model EGY-HQGM2016, geoid/quasigeoid separation and the final hybrid gravimetric geoid model HGM2016.

Table 3: Statistics of height anomalies, geoid-to-quasigeoid separation and geoid heights [m]

	Min	Max	Mean	st. dev.
Hybrid gravimetric quasigeoid model (EGY-HQGM2016)	7.678	21.098	14.155	2.253
Geoid-to-quasigeoid separation	-0.392	0.009	-0.016	0.028
Hybrid gravimetric geoid model (HGM2016)	7.677	21.095	14.139	2.534

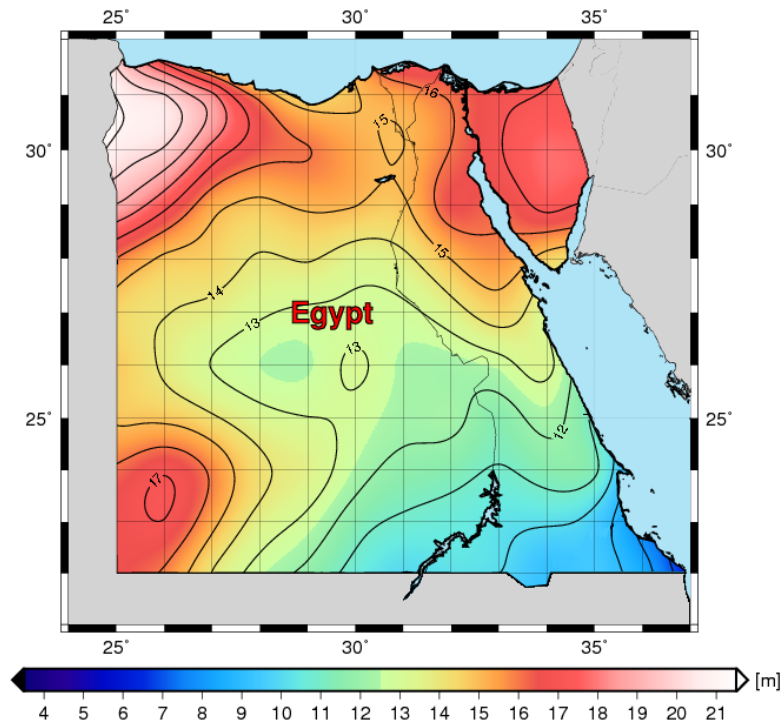


Figure 4: The hybrid gravimetric geoid model HGM2016.

4 Accuracy assessment of the developed hybrid gravimetric geoid model EGY-HGM2016 using the GPS/levelling data

In order to check the quality of the developed HGM2016 model, the geoid heights obtained from our model have been compared with the corresponding ones determined by GPS/levelling. The differences here are given on the form

$$\Delta N = N_{\text{HGM2016}} - N_{\text{GPS/levelling}} \quad [6]$$

The statistics concerning Eq.6 are indicated in Table 6 in terms of st. dev. of the differences between the geoid heights of HGM2016 and the corresponding from GPS/levelling data as obtained from of HARN network (see Figure 1).

The statistics given in Table 6 consist of two main parts regarding the comparison between geoid heights of HGM2016 with the corresponding ones from GPS/levelling data on the one hand, and with the corresponding ones from EGM2008 and GECO gravity models on the other hand.

The statistics show that the geoid heights differences between the 17 GPS/levelling points of HARN and the developed HGM2016 model provide reduced st. dev. of about 19.7 cm and of about 48 cm and 36 cm in case of EGM2008 and GECO, respectively. This emphasizes that the EGY-HGM2016 model provide improved geoid heights over Egypt than those given by EGM2008 and GECO models.

Table 6: Statistics of differences between the estimated HGM2016 for Egypt and the corresponding ones from the GPS/levelling data, EGM2008 and GECO gravity models [m].

Statistics	Min	Max	Mean	st. Dev.
$N_{17 \text{ GPS/levelling HARN}}$	9.779	19.33	14.458	2.743
N_{HGM2016}	9.856	19.613	14.469	2.795
N_{EGM2008}	9.772	19.498	14.186	2.833
N_{GECO}	9.75	19.53	14.179	2.89
$N_{17 \text{ GPS/levelling HARN}} - N_{\text{HGM2016}}$	-0.409	0.309	-0.006	0.197
$N_{17 \text{ GPS/levelling HARN}} - N_{\text{EGM2008}}$	-0.708	1.380	0.272	0.480
$N_{17 \text{ GPS/levelling HARN}} - N_{\text{GECO}}$	-0.454	0.822	0.278	0.362

5. Conclusion

In this study, hybrid gravimetric geoid-quasigeoid model HGM2016 has been developed by means of least-squares collocation method and remove-compute-restore process over Egypt. Datasets from heterogeneous terrestrial and marine gravity data as well as GPS/levelling data have been used during our modelling process. The GOCE-based model GO_CONS_GCF_2_SPW_R4 up to d/o 200 has been chosen to recover the long wavelength component of the gravity signal in the hybrid gravimetric quasigeoid modelling process, since it approximates the gravity field well the over Egypt. Moreover, short gravity signal from d/o 201 to d/o 720 has been compensated using EGM2008 model to create modified GOCE.EGM model from d/o 2 to d/o 720. We have performed this step in order to strengthen the medium-to-short wavelength of the gravity spectrum when modelling the hybrid gravimetric quasigeoid heights over Egypt. The d/o 720 has been selected here because beyond this degree the EGM2008 is solely based on topography.

The accuracy of the developed hybrid gravimetric geoid model HGM2016 has been checked using 17 point stations obtained from GPS/levelling data, and EGM2008 and GECO gravity models. The statistics in terms of st. dev. of the differences show that our developed model provides improved geoid heights by a factor of about 2 – 2.5 compared to EGM2008 and GECO gravity models when using the 17 GPS/levelling HARN stations.

This emphasizes that the HGM2016 model provide more improvements and reliable geoid heights over Egypt with respect to EGM2008 and GECO gravity models.

Acknowledgement: The computations of HGM2016 were carried out using the software modules of GRAVSOFT (Forsberg and Tscherning, 2008). The spatial representations of the results have been plotted using the GMT5 (Generic Mapping Tools) software (Wessel et al., 2013).

6. References

- Abd-Elmotaal, H. (2008). Gravimetric geoid for Egypt using high-degree tailored reference geopotential model, NRIAG Journal of Geophysics special issue. pp. 507-531.
- Alnaggar, D. (1986). Determination of the geoid in Egypt using heterogeneous geodetic data, PhD dissertation, Faculty of Engineering, Cairo University, Egypt.

- Andersen, O., and Knudsen, P. (2013). The DTU13 MSS New global Mean sea surface from 20 years of satellite altimetry, Poster presented at the IAG Scientific Assembly 2013, Potsdam, 1- 6 September 2013.
- Dawod, G. (1998). A national gravity standardization network for Egypt, PhD dissertation, Faculty of Engineering at Shoubra, Zagazig University, Egypt.
- Dawod, G. (2008). Towards the redefinition of the Egyptian geoid: Performance analysis of recent global geoid and digital terrain models, *Journal of Spatial Science*, V 53, Issue 1, 31-42, <http://dx.doi.org/10.1080/14498596.2008.9635133>.
- Denker, H., Torge, W., Wenzel, G., Ihde, J., and Schirmer, U. (2000) Investigation of different methods for the combination of gravity and GPS/levelling data. In: Schwarz K-P (ed) *Geodesy beyond 2000—the challenges of the first decade*, International Association of Geodesy Symposia, vol 121. Springer, Berlin Heidelberg New York. pp 137–142.
- El-Ashquer, M., Elsaka, B., and El-Fiky, G. (2016). On the accuracy assessment of the latest releases of GOCE satellite-based geopotential models with EGM2008 and terrestrial GPS/levelling and gravity data over Egypt, *International Journal of Geosciences* (submitted).
- El-Tokhy, M. (1993) *Towards the Redefinition of the Egyptian Geodetic Control Networks: Geoid and Best Fitting Reference Ellipsoid by Combination of Heterogeneous Data*, Ph.D. Thesis, Faculty of Engineering, Ain Shams University, Egypt.
- Forsberg, R., and Tscherning, C. (2008). An overview manual for the GRAVSOFT Geodetic Gravity Field Modelling Programs, 2. Edition, National Space Institute (DTU-Space), Denmark, August.
- Gatti, A., Reguzzoni, M., Migliaccio, F. & Sansò, F. (2014). Space-wise grids of gravity gradients from GOCE data at nominal satellite altitude. 5th International GOCE User Workshop. Paris (UNESCO), France. 25-28 November 2014.
- Hofmann-Wellehof, B., and Moritz, H. (2005). *Physical Geodesy*, Springer-Verlag Wien. Printed in Austria.
- Knudsen, P. (1987). Estimation and Modelling of the Local Empirical Covariance Function using gravity and satellite altimeter data, *Bulletin Geodesique*, vol. 61, pp. 145–160.
- Kuroishi, Y. (2001b). A new geoid model for Japan, JGEOID2000, In: Sideris M (ed) *Gravity, geoid and geodynamics 2000*, International Association of Geodesy Symposia, vol 123. Springer, Berlin Heidelberg New York, pp 329–333.
- Milbert, D.G. (1995). Improvement of a high resolution geoid height model in the Unites States by GPS height on NAVD88 benchmarks, *Bull d'Informations 77 and IGeS Bull 4, Special Issue, New Geoid in the Worlds*, Milan, Toulouse, 13-16.
- Nassar, M., El-Maghraby, M., El-Tokhey, M., and Issa, M. (2002). Development of a New Geoid Model for Egypt (ASU2000 Geoid) Based on the ESA High Accuracy Reference Network (HARN), *Scientific Engineering Bulletin*, Faculty of Engineering ,Ain Shams University, 35, (4).
- Pavlis, N.K., Holmes, S.A., Kenyon, S.C., and Factor, J.K. (2012). The development and evaluation of the earth gravitational model 2008 (EGM2008). *J Geophys. Res.* 117(B04406): 1–38.

- Schwarz, K-P., Sideris, M.G., and Forsberg, R. (1990). Use of FFT methods in Physical Geodesy, *Geophysical Journal International*. 100: 485 – 514.
- Smith, D.A., and Milbert, D.G. (1999). The GEOID96 high resolution geoid model for the United States, *J Geod*, 73:219–236.
- Smith, D.A., Roman, D.R. (2001). GEOID99 and G99SSS: 1-arcminute geoid models for the United States, *J Geod*, 75:469–490.
- Tscherning, C.C., Rapp, R.H. (1974). Closed Covariance Expressions for Gravity Anomalies, Geoid Undulations, and Deflections of the Vertical Implied by Anomaly Degree-Variance Models, Reports of the Department of Geodetic Science No. 208, The Ohio State University, Columbus, Ohio.
- Wessel, P., W. H. F. Smith, Scharroo, R., Luis, J. F. and Wobbe, F., (2013). Generic Mapping Tools: Improved version released, *EOS Trans. AGU*, 94, pp. 409–410.